

Supplementary Information: ¹H-NMR characterization of MA-Chol, degradability assessment of MA-Chol in 10% FBS condition, siRNA encapsulation efficiency of SLNPs, serum stability of siRNA@SLNPs, time-course colloidal stability of siRNA@SLNPs in 10% FBS condition, comparison of siRNA encapsulation efficiency in SLNPs and DC-Chol/DOPE liposomes, intracellular uptake of TAMRA-siRNA@SLNPs by U87MG cells, tumor weights and changes in body weights in response to *in vivo* treatment with siRNA@SLNPs, and hemolysis assay.

Supplementary Information

Mono-arginine Cholesterol-based Small Lipid Nanoparticles as a Systemic siRNA Delivery Platform for Effective Cancer Therapy

Jinju Lee,[†] Phei Er Saw,[‡] Vipul Gujrati,[‡] Yonghyun Lee,[‡] Hyungjun Kim,[‡] Sukmo Kang,[‡] Minsuk Choi,[‡] Jae-Il Kim[†] and Sangyong Jon^{‡,*}

[†]School of Life Science, Gwangju Institute of Science and Technology, 123 Cheomdangwagi-ro, Gwangju 500-712, Republic of Korea. [‡]KAIST Institute for the BioCentury, Department of Biological Sciences, Korea Advanced Institute of Science and technology (KAIST), 291 Daehak-ro, Daejeon 305-701, Republic of Korea.

Table of Contents

1. Figure S1. ¹H-NMR characterization of MA-Chol in DMSO-d⁶.
2. Figure S2. Evaluation of degradability of MA-Chol in 10% FBS.
3. Figure S3. Encapsulation efficiency of siRNA within SLNPs.
4. Figure S4. Serum stability of siRNA@SLNPs.
5. Table S1. Colloidal stability of siRNA@SLNPs in 10% FBS condition.

6. Figure S5. Comparison of siRNA encapsulation efficiency in SLNPs and DC-Chol/DOPE-based lipid nanoparticles.
7. Figure S6. Intracellular uptake of TAMRA-siRNA@SLNPs by U87MG cells.
8. Figure S7. Tumor weights and changes in body weights in response to *in vivo* treatment with siRNA@SLNPs.
9. Figure S8. Hemolysis study of SLNPs and DC-Chol/DOPE-based lipid nanoparticles.

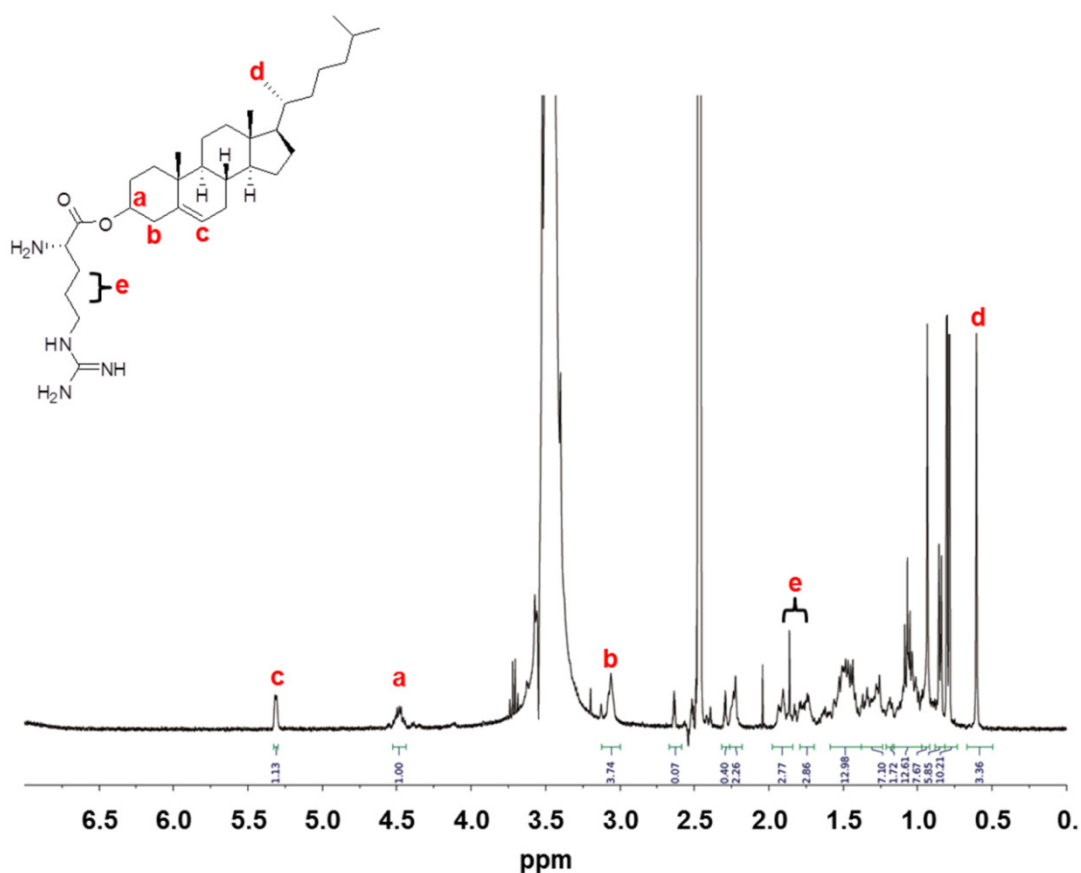


Figure S1. ^1H -NMR characterization of MA-Chol in DMSO-d_6 .

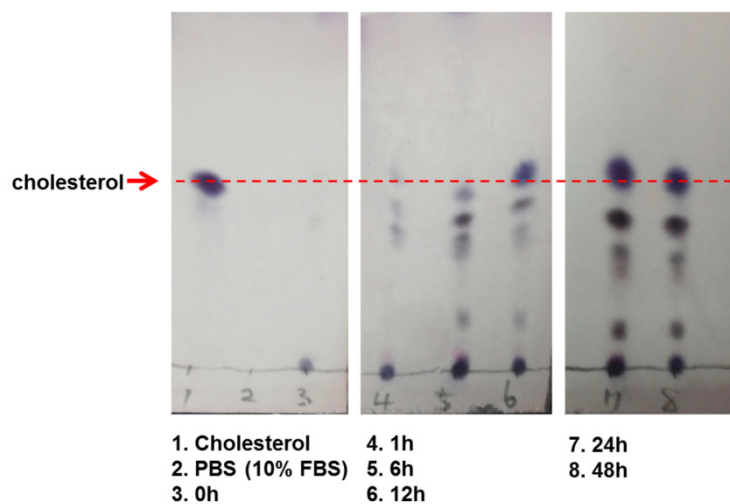


Figure S2. Evaluation of degradability of MA-Chol in 10% FBS. MA-Chol (10 mg/mL) was incubated in PBS (pH 7.4) containing 10% FBS at 37°C and aliquots were collected at each time points. Each aliquot (100 µL) was mixed with 400 µL of chloroform to extract organic compounds. The collecting chloroform layer was evaporated to concentrate the solvent. The remaining crude concentrate was developed in chloroform : methanol = 15 : 1 (v/v) by thin layer chromatography (TLC) and further stained with p-anisaldehyde solution for detection.

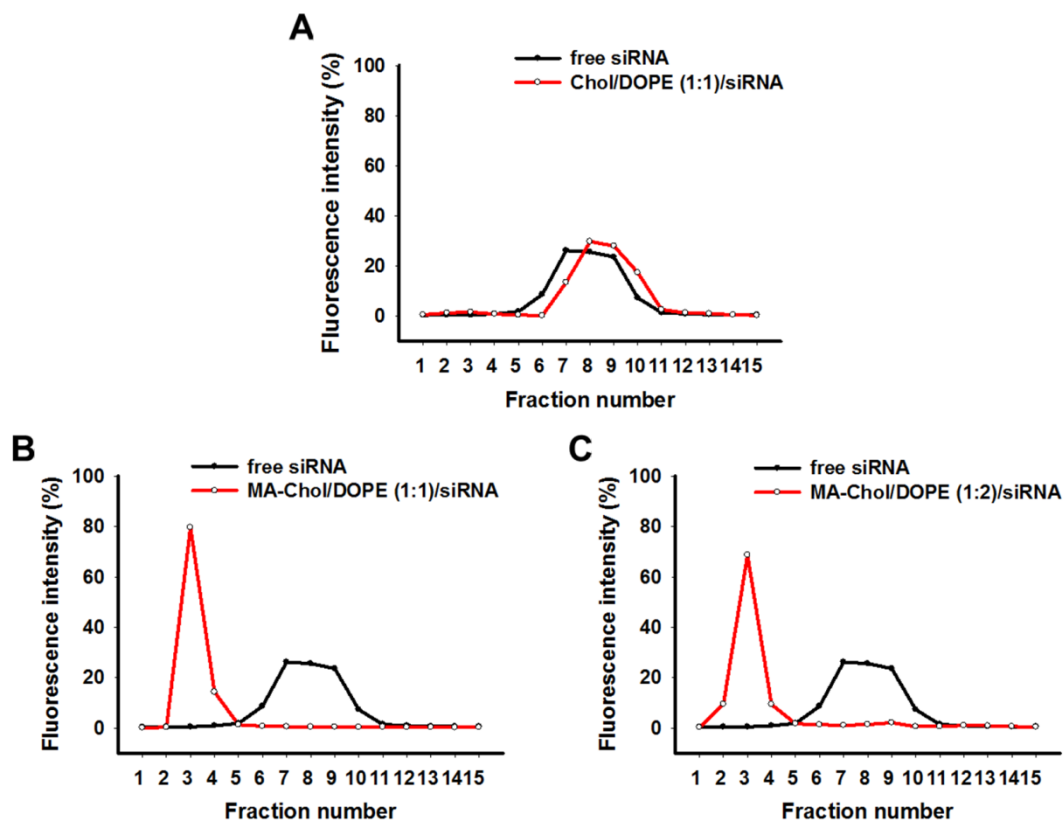


Figure S3. siRNA encapsulation efficiency of SLNPs. Encapsulation efficiency of non-modified cholesterol/DOPE liposomes and MA-Chol/DOPE (1:1 and 1:2) liposomes with siRNA were analyzed using OliGreen (Invitrogen) according to manufacturer's protocol. Total 4 μ mol lipid of Chol/DOPE or MA-Chol/DOPE liposomes were rehydrated with 3 nmol siRNA and the resulting liposome solutions were loaded onto Sepharose CL-4B column. (a) Any siRNA was encapsulated in Chol/DOPE liposomes. (b) MA-Chol/DOPE (1:1) and (c) MA-Chol/DOPE (1:2) liposomes revealed 100% of siRNA encapsulation efficiency.

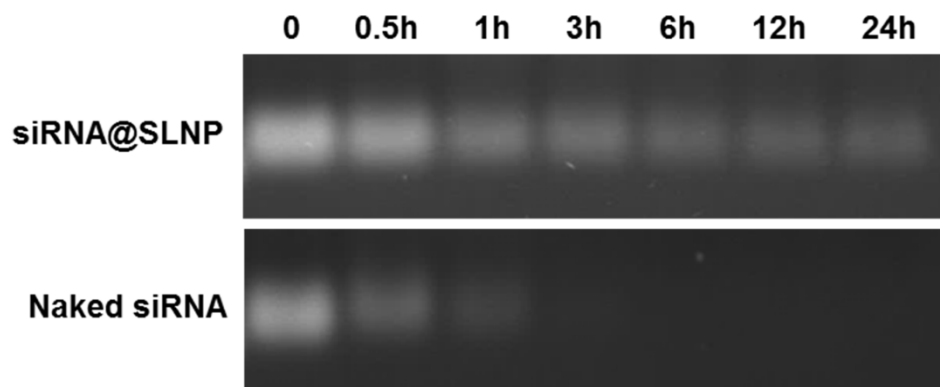


Figure S4. Serum stability of siRNA@SLNPs. Equivalent amount of siRNA and siRNA@SLNPs were incubated with 30% fetal bovine serum (FBS)-conditioning buffer at 37°C for 0.5, 1, 3, 6, 12, and 24 h. After indicated incubation times, aliquots containing 1 μ g siRNA of each sample were visualized by 12% agarose gel electrophoresis. While naked siRNA showed rapid degradation within 3 h, siRNA encapsulated within SLNPs remained 75% intact for up to 6 h and 40% of siRNA was stable for up to 24 h.

Table S1. Colloidal stability of siRNA@SLNPs in 10% FBS condition. The integrity of siRNA@SLNPs upon incubation in PBS containing 10% FBS at 37°C was evaluated with respect to size and zeta potential at predetermined time points (0, 1, 3, 6, 12, and 24 h).

Time (h)	0	1	3	6	12	24
Size (nm)	49 ± 5.2	47 ± 8.0	49 ± 7.6	49 ± 5.8	59 ± 6.0	80 ± 7.3
Zeta potential (mV)	0.12 ± 1.8	0.15 ± 2.3	0.67 ± 2.3	1.3 ± 1.8	4.2 ± 1.3	8.9 ± 2.7

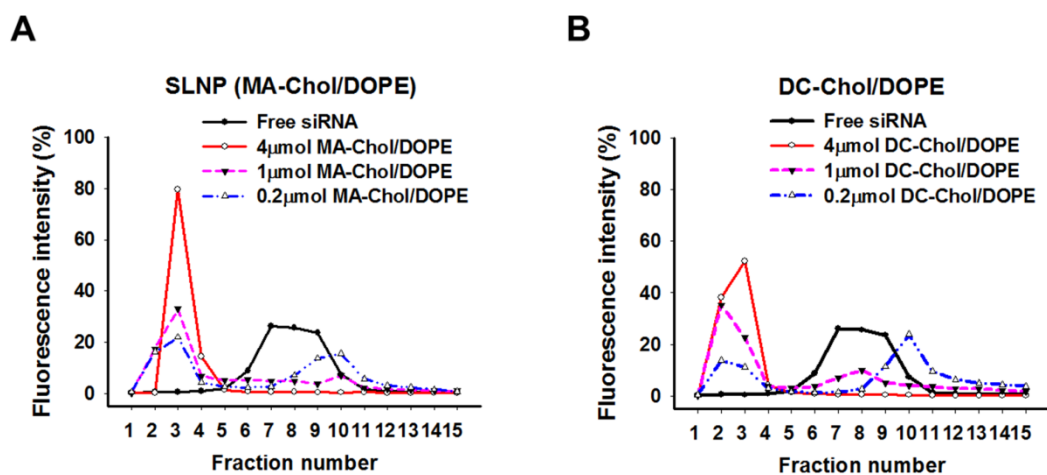


Figure S5. Comparison of siRNA encapsulation efficiency in SLNPs and DC-Chol/DOPE liposomes. SLNPs comprised of MA-Chol/DOPE (1:1) and DC-Chol/DOPE (1:1) liposomes were analyzed with respect to siRNA encapsulation efficiency as a function of lipid concentration. Both SLNPs and DC-Chol/DOPE liposomes were shown to have similar complexation ability and encapsulation efficiency for siRNA.

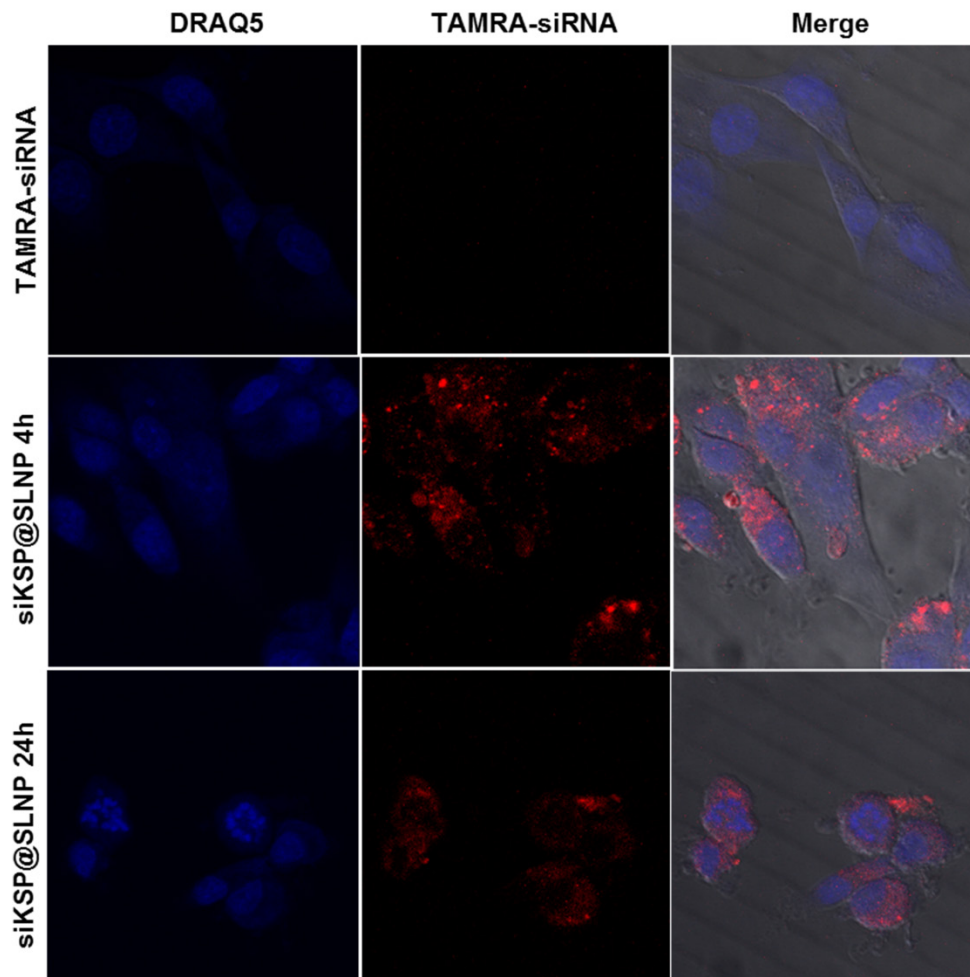


Figure S6. Intracellular uptake of TAMRA-siKSP@SLNPs by U87MG cells. Cells were treated with TAMRA-siKSP(100 nM)@SLNPs for 4 h and monitored for 24 h using a confocal microscope. At 24 h post transfection, many cancer cells started to become circularized and fragmented form of nucleus was observed.

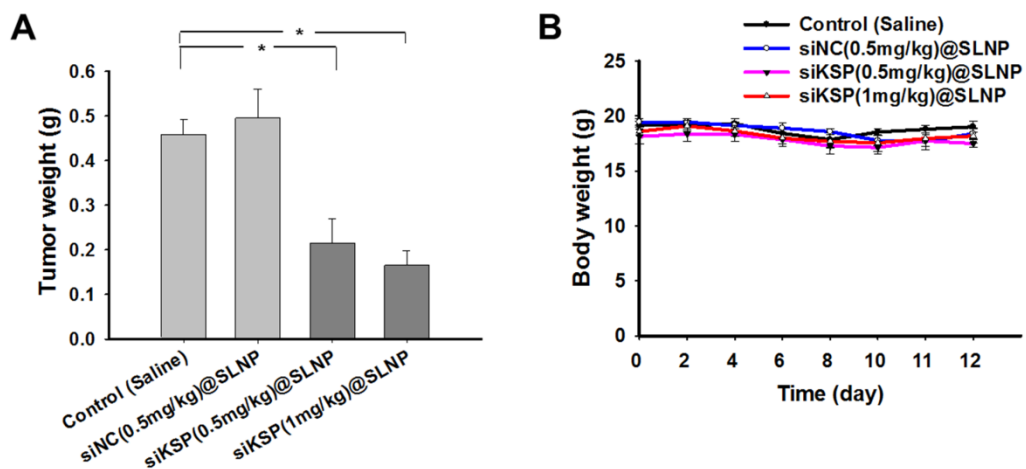


Figure S7. Tumor weights and changes in body weight in response to *in vivo* treatment with siKSP@SLNPs in PC-3 tumor-bearing nude mice. * indicates $p < 0.05$.

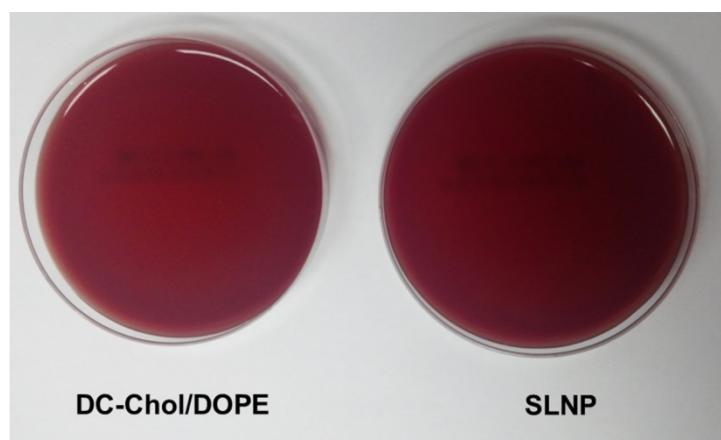


Figure S8. Hemolysis study of SLNPs and DC-Chol/DOPE-based lipid nanoparticles. Hemolysis study was performed by plating SLNPs (only vehicle) or DC-Chol/DOPE-based lipid nanoparticles on horse blood agar plates under standard conditions. Both lipid nanoparticle systems did not induce hemolysis.